



## CONFINEMENT OF CONCRETE OF R/C MEMBERS UNDER VARYING AXIAL LOAD

D. KATO, Y. HONDA, H. SUZUKI and J. SHIBA

Department of Architecture, Faculty of Engineering, Niigata University  
8050 Ikarashi 2-nocho, Niigata, 950-21, Japan

### ABSTRACT

The objective of this paper is to propose an evaluating equation for deformation capacities determined by flexural failure, which is caused by the compressive failure of the core concrete. The effects of the compressive failure of the core concrete become significant in case of corner columns subjected to varying high axial load. Therefore, these problems are discussed paying special attention to the effects of the varying axial load. Core sections with the same amount of longitudinal reinforcement both in tension and compression were studied. The rigid-plastic relation was assumed for steel bars and the stress block relation without energy dissipation under cyclic loading was assumed for concrete. Under these assumptions the evaluating equation of ultimate curvature  $\phi_u$  of columns subjected to not only constant axial load but varying axial load was developed. The idea of equivalent axial load was introduced to apply the evaluating equation to specimens with varying axial load. Deformation capacity was defined as the deformation when the restoring force degraded to  $\alpha$  ( $\alpha=0.7 - 1.0$ ) of the maximum strength. The evaluating equation of  $\phi_u$  for each degradation ratio  $\alpha$  was developed using 104 specimens with constant axial load and 22 specimens with varying axial load. Note that only specimens whose deformation capacities were determined by flexural failure were used. Consequently, the proposed equivalent axial load ratio and the evaluating equation for deformation capacities determined by flexural failure were found to be effective.

### KEYWORDS

Reinforced concrete column; deformation capacity; varying axial load; concrete model; core concrete.

### INTRODUCTION

Recent earthquake resistant design concept of structures places explicit emphases on the inelastic deformation

capacity in addition to the previously accepted resisting capacity. Deformation capacities of reinforced concrete members are determined by shear failure, bond failure, flexural failure or buckling of main bars after flexural yielding of the sections. In the design guidelines for earthquake resistant reinforced concrete buildings based on ultimate strength concept proposed by Architectural Institute of Japan (AIJ, 1990), practical design equations for ductility are presented for the first two failure mechanisms. However, only ambiguous specification for arranging methods are regulated for the last two failure mechanisms.

The objective of this paper is to propose an evaluating equation for deformation capacities determined by flexural failure, which is caused by the compressive failure of the core concrete. The effects of compressive failure of the core concrete become significant for corner columns subjected to varying high axial load. Therefore, these problems are discussed paying special attention to the effects of the varying axial load.

## DEFORMATION CAPACITY DETERMINED BY FLEXURAL FAILURE

### Evaluating equation of deformation capacity determined by flexural failure

An evaluating equation for deformation capacities determined by flexural failure, which is caused by the compressive failure of the core concrete, is discussed in this section. The compressive failure of the core concrete become significant for corner columns subjected to varying high axial load. Therefore these problems are discussed paying special attention to the effects of the varying axial load.

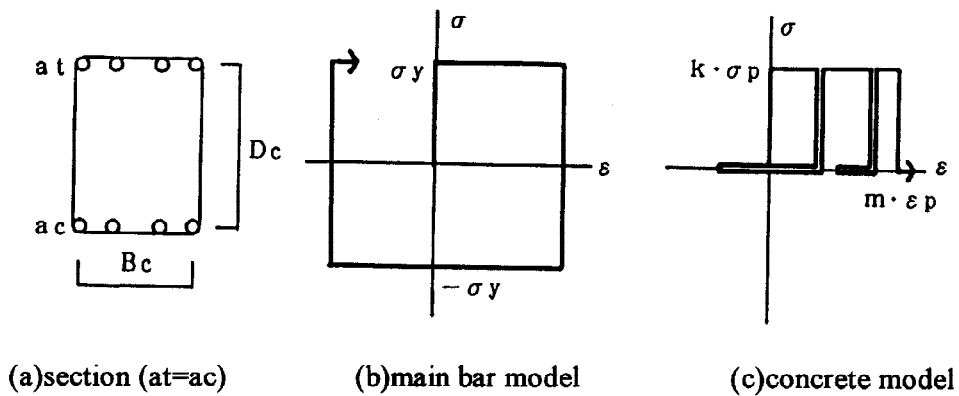


Fig.1 Assumptions of section studied and material models

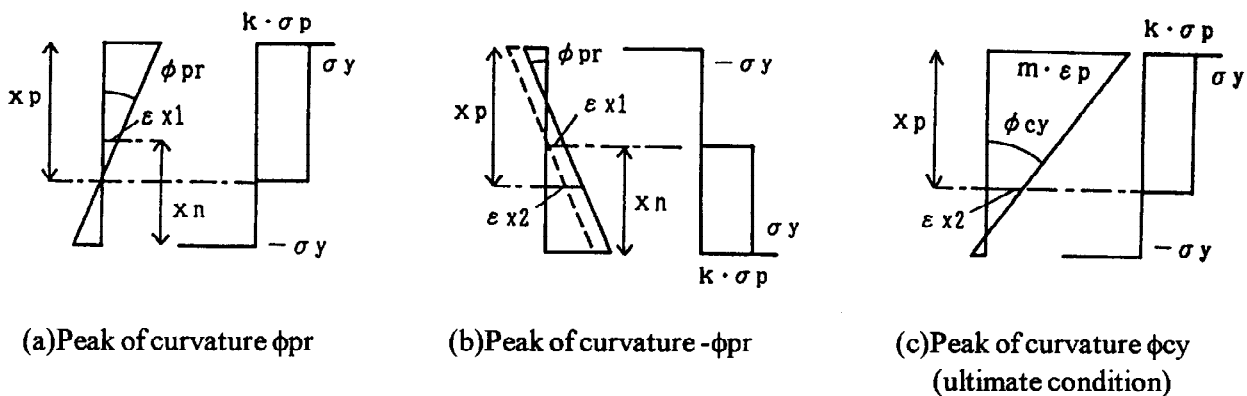


Fig.2 Transition of strain and stress distributions of section subjected to varying axial load and moment

Figure 1 shows the studied sections and the assumptions of material models. Core sections with the same amount of longitudinal reinforcement both in tension and compression ( $a_t=a_c$ ) were studied. The rigid-plastic relation was assumed for steel bars and the stress block relation without energy dissipation under cyclic loading was assumed for concrete. The symbols  $k$  and  $m$  denote the coefficients of the stress block for stress and strain, respectively. Figure 2 shows the transitions of strain and stress distributions of the section subjected to varying axial load and moment reversals. Figure 2(a) shows the condition at the curvature of  $\phi_{pr}$  with monotonic loading. The strain and stress distributions at the curvature of  $-\phi_{pr}$  after the reversed loading are shown in Fig. 2(b) by solid lines. The dashed line in this figure represents the imaginary condition with monotonic loading, which indicates that the axial strain of the section is increased by reversed loading. Figure 2(c) illustrates an ultimate condition at the curvature of  $\phi_{cy}$  after one moment reversal at the curvature of  $\pm\phi_{pr}$  (Figs. 2(a)(b)). The accumulated strain of the compressive concrete in the section can be observed. The ultimate curvature  $\phi_u$  can be expressed as Eq. (1) on a supposition that  $\phi_{pr}=\phi_{cy}(=\phi_u)$ .

$$\phi_u / (m \epsilon_p / D_c) = \begin{cases} k / \eta_p & (k / (1 + \gamma) > \eta_p > 0) \\ k / ((3 + 2\gamma)\eta_p - 2k) & (k > \eta_p > k / (1 + \gamma)) \end{cases} \quad (1)$$

$$\eta_p = N_p / (D_c B_c \sigma_p) \quad \eta_n = N_n / (D_c B_c \sigma_p) \quad \gamma = \eta_n / \eta_p \quad (\gamma > 0)$$

where,  $N_p$  and  $N_n$  denote the maximum and minimum axial loads (positive value for compression). Other symbols are shown in Fig. 2. The term "normalized ultimate curvature" refers to  $\phi_u / (\epsilon_p / D_c)$  in this report.

Figure 3 shows calculated relations between normalized ultimate curvatures and maximum varying axial loads using Eq. (1) ( $k=2/3$ ,  $m=1$ ). Three values 0, 0.5 and 1.0 for  $\gamma$  were chosen for examples. This figure indicates that no effects of varying axial load on ultimate curvature are expected when the axial load ratio is lower than 0.33. On the other hand, effects increase with the increasing value of the axial load ratio after that of 0.33. The symbols  $\eta_p$  and  $e\eta$  in Fig. 3 represent the maximum axial loads of two members with the same normalized ultimate curvature. Considering that the ultimate curvature of the member with varying axial load ( $\gamma=0$ ), the maximum value of which is  $\eta_p$ , is as same as that with constant axial load of  $e\eta$  ( $\gamma=1$ ), it is concluded that the two members have the same deformation capacity. Namely the axial load ratio  $e\eta$  can be used to calculate the deformation capacity of

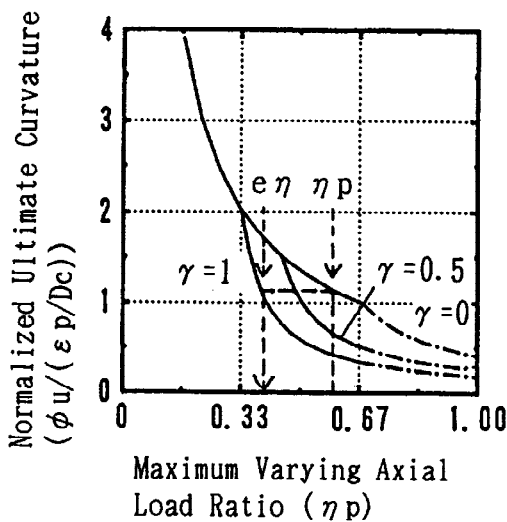


Fig. 3 Effects of varying axial load on relations between axial load and ultimate curvature

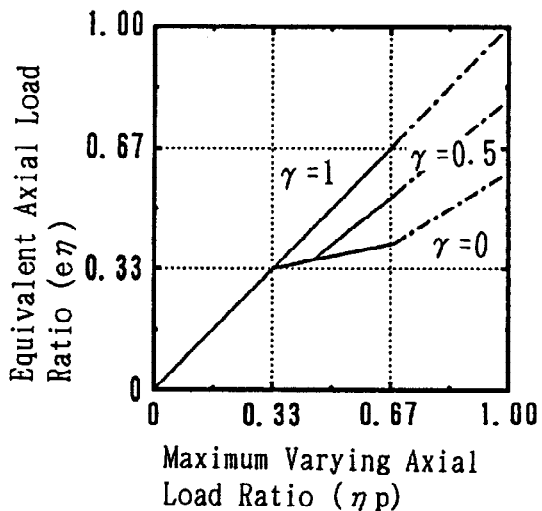


Fig. 4 Relations between varying axial load and equivalent axial load

the member with varying axial load, the maximum value of which is  $\eta p$ . The term "equivalent axial load" refers to  $e \eta$  in this study.

The equivalent axial load is expressed by Eq. (2), which was derived using Eq. (1)

$$e \eta = \begin{cases} \eta p & 1/3 > \eta p > 0 \\ \eta p / 5 + 4/15 - \eta_s & (> 1/3) \quad 2/3 / (1 + \gamma) > \eta p > 1/3 \\ \eta p (3 + 2\gamma) / 5 - \eta_s & (> 1/3) \quad 2/3 > \eta p > 2/3 / (1 + \gamma) \end{cases} \quad (2)$$

where,  $\eta_s$  denotes the contribution of the axial load ratio supported by longitudinal reinforcement located at the center of the section. Figure 4 shows the relations between equivalent axial load and maximum varying axial load.

### Concrete model used

In this study the concrete model proposed as a result of the New RC Projects was used for core concrete confined by square hoop reinforcement. This model was developed to match with a variety of experimental data conducted not only during the New RC Projects but by overseas researchers. The maximum strength of concrete and transverse reinforcement used in examined specimens was 132 and 1109 MPa, respectively. The maximum stress  $\sigma_p$  and the strain at the maximum point  $\epsilon_p$  of confined square core concrete are expressed as follows.

$$\sigma_p = \sigma_c + \kappa \rho_w h \sigma_{wy} \quad (\sigma_{wy} < 687 \text{ MPa}) \quad (3)$$

$$\epsilon_p = \begin{cases} \epsilon_c (1 + 4.7(K-1)) & (K < 1.5) \\ \epsilon_c (3.35 + 20(K-1.5)) & (K > 1.5) \end{cases} \quad (4)$$

$$\begin{aligned} \sigma_c &= \sigma_B \\ \kappa &= 11.5(\phi w / C)(1 - 0.5 S_w / D_c) \\ \epsilon_c &= 0.93(\sigma_B)^{1/4} 10^{-3} \\ K &= \sigma_p / \sigma_c \end{aligned}$$

where,  $\sigma_B$  denotes concrete strength (MPa),  $C$  denotes length between effective supports of hoop,  $\sigma_c$  denotes maximum strength of plain concrete (MPa),  $\epsilon_c$  denotes axial strain at maximum point of plain concrete,  $\rho_w h$  denotes volumetric ratio of reinforcement to concrete core,  $D_c$  denotes core depth (mm),  $\sigma_{wy}$  denotes yielding strength of hoop (MPa),  $\phi w$  and  $S_w$  denote diameter and spacing of hoop (mm).

### DEFORMATION CAPACITY DETERMINED BY SHEAR FAILURE

Figure 5 shows an assumed relation between load and deflection angle of a member whose deformation capacity is determined by shear failure. Thick dashed line in the figure represents the potential shear strength calculated using Eq. (5) shown below, which was proposed by Architectural Institute of Japan (1990). The potential shear strength is the function of the deflection angle of the member ( $R_p$ ) and the point A in Fig. 5 represents the deformation capacity defined as the deflection angle when restoring force degrades to calculated flexural strength  $Q_f$ . Assuming  $Q_f$  to be 80% of the maximum strength  $Q_{max}$ , the point A represents the deformation capacity defined as the deflection angle when restoring force degrades to 80% of the maximum strength. In the same way deformation capacities can be obtained for arbitrary strength degradation ratios  $\alpha$ .

$$Q_s = b j t p_w \sigma_{wy} \cot \phi + \tan \theta (1 - \beta) b D v \sigma_B / 2 \quad (p_w \sigma_{wy} < v \sigma_B / 2) \quad (5)$$

$$\tan\theta = \sqrt{\{(H/D)^2 + 1\}} - H/D$$

$$\beta = \frac{\{(1+\cos^2\phi)pw \sigma_{wy}\}}{(1-1.5 R_p) v_0} \quad \begin{matrix} (\sigma_{wy} < 25 \sigma_B) \\ (0 < R_p < 0.05) \end{matrix}$$

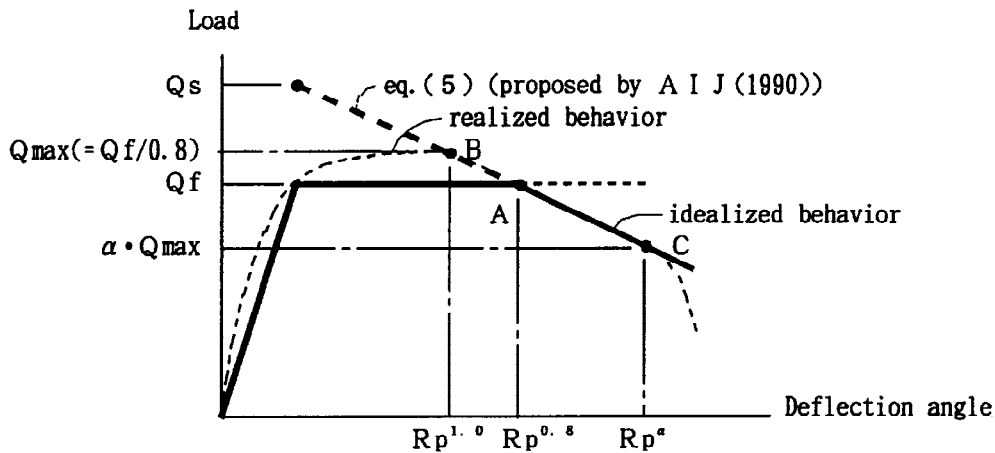
$$v = \begin{cases} 0.25 v_0 & (0.05 < R_p) \end{cases}$$

$$v_0 = 1.72 \sigma_B^{-0.33} \quad (\text{unit of } \sigma_B : \text{MPa})$$

$$\cot\phi = \min \{ \cot\phi_1, \cot\phi_2, \cot\phi_3 \}$$

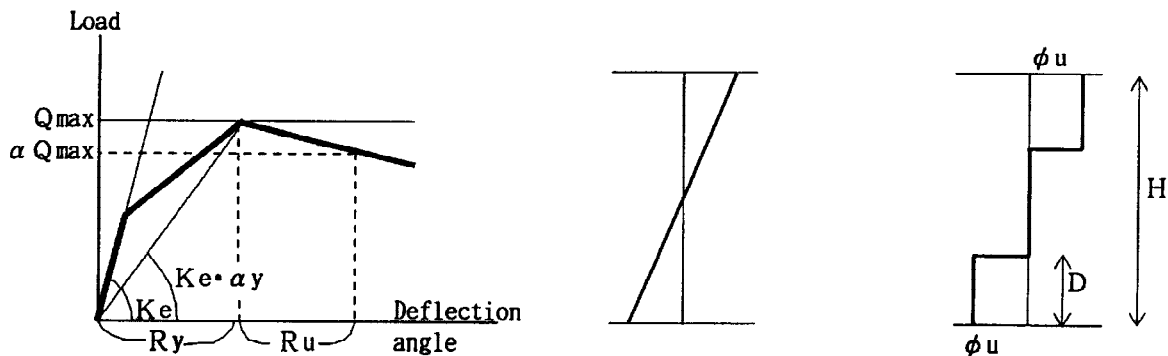
$$\cot\phi_1 = \frac{jt}{(D \tan \theta)}$$

$$\cot\phi_2 = \sqrt{v \sigma_B / (pw \sigma_{wy})} - 1$$



$Q_s$  : calculated potential shear strength  
 $Q_f$  : calculated flexural yielding strength  
 $Q_{max}$  : realized maximum flexural strength (assumed to be  $Q_f/0.8$ )  
 $R_p^\alpha$  : calculated deformation capacity determined by shear failure (deformation capacity is defined as deformation when restoring force degrades to  $\alpha$  of maximum strength)

Fig. 5 Assumed relation between load and displacement of a member whose deformation capacity is determined by shear failure



(a) Plastic deformation (b) Moment distribution (c) Plastic curvature distribution

Fig. 6 Assumption of plastic deformation and plastic curvature distribution

$$\cot\phi_3 = \begin{cases} 2 - 50 R_p & ( 0 < R_p < 0.02 ) \\ 1 & ( 0.02 < R_p ) \end{cases}$$

where,  $b$ ,  $D$ ,  $j_t$  and  $H$  represent width, depth, distance between longitudinal main bars and span length and  $p_w$  denotes shear reinforcement ratio.

The calculated flexural strength  $Q_f$  was obtained using Eq. (6) expressed as follows.

$$M_f = \begin{cases} 0.8 \text{ at } \sigma_y D + 0.5 N D (1 - N / (b D \sigma_B)) & (N < 0.4 b D \sigma_B) \\ 0.8 \text{ at } \sigma_y D + 0.12 b D^2 \sigma_B & (N > 0.4 b D \sigma_B) \end{cases} \quad (6)$$

where,  $A$  and  $\sigma_y$  denote area and yield strength of tensile longitudinal main bars,  $N$  denotes the axial load.

## EXAMINATION WITH TEST RESULTS

### Examined specimen and evaluation of plastic curvature

104 specimens with constant axial load and 22 specimens with varying axial load, shown by Kato *et.al.* (1995) were used for this study. The ranges of variables are shown in Table 1. Figure 6 shows the assumption of plastic deformation and plastic curvature distribution. The plastic deformation  $R_u$  was obtained by subtracting yield deformation  $R_y$  from total deformation as shown in Fig. 6(a) and expressed as Eq. (7). The degradation ratio of yield stiffness to elastic stiffness  $\alpha_y$  was derived as an experimental equation and popularly used in Japan.

$$\begin{aligned} R &= R_y + R_u & (7) \\ Q_{\max}/R_y &= \alpha_y K_e \\ \alpha_y &= (0.043 + 1.64 n_{pt} + 0.043 r_s + 0.33 \eta_o) (d/D)^2 \end{aligned}$$

where,  $K_e$  is the elastic stiffness,  $n$ ,  $p_t$ ,  $r_s$ ,  $\eta_o$  and  $d$  denote young modulus ratio of steel to concrete, area ratio of tensile longitudinal main bars to gross section, shear span ratio to section depth, axial load ratio to gross section and effective depth of the section.

The plastic curvature  $\phi_u$  was obtained supposing the plastic curvature inside the hinge region was constant as shown in Fig. 6(c) and expressed as Eq. (8).

Table 1. Range of properties of examined 126 specimens

concrete strength	22.7 - 122 MPa
main bar strength	338 - 999 MPa
hoop strength	274 - 1766 MPa
maximum axial load ratio	-0.26 - 1.10

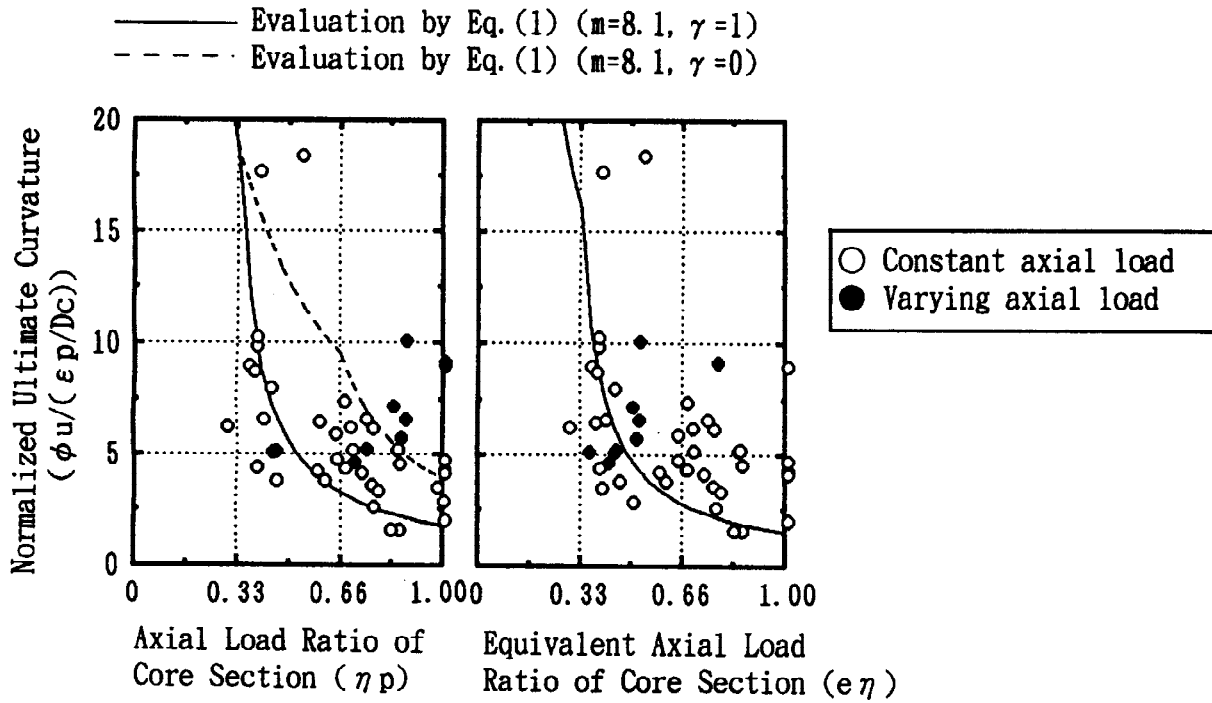
$$\phi_u = R_u / \{ D ( 1 - D / H ) \}$$

$$( D < H/2 )$$

(8)

Comparison between calculation and observation

Figure 7 shows the relations between observed ultimate curvatures and axial load ratios of core sections. The coefficient of the stress block  $k$  was assumed to be  $2/3$  in this study and the coefficient  $m$  was chosen to match the



(a) with maximum axial load

(b) with equivalent axial load

Fig. 7 Relations between axial load ratio of core sections and normalized ultimate curvature (strength degradation ratio  $\alpha=0.8, k=2/3$ )

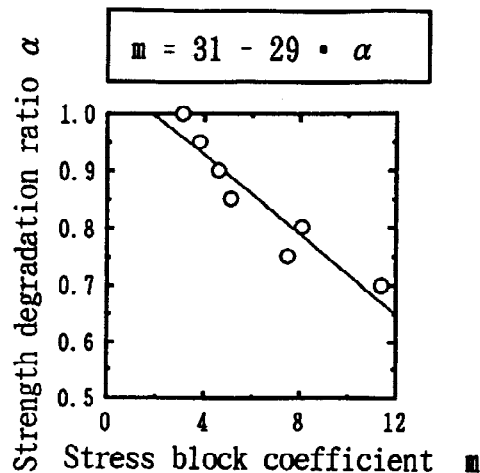


Fig. 8 Relations between strength degradation ratio  $\alpha$  and stress block coefficient  $m$  ( $k = 2/3$ )

analytical results with the observation. The observed ultimate point was defined as the point when the restoring force degraded to 80% of the maximum load ( $\alpha = 0.8$ ). Figure 7(a) shows relations with maximum axial loads and Fig. 7(b) shows that with equivalent axial loads. The curvature was normalized by  $\epsilon_p/D_c$  in these figures. It must be noted that only specimens whose deformation capacities were determined by flexural failure was illustrated in the figures. In other words, specimens whose deformation capacities calculated using Eq. (1) were smaller than those calculated using the philosophy shown by Fig. 5 were chosen. However, because the coefficient of the stress block  $m$  in Eq. (1) was unknown and would be obtained to match with the observation, some iterative procedures were necessary.

In Fig. 7(a) calculated relations using Eq. (1) are illustrated with two different values of  $\gamma$ ;  $\gamma=1$  (constant axial load) and  $\gamma=0$  (varying axial load, the minimum load = 0). The coefficient of the stress block  $m$  was chosen to match the analytical results with the observation by the method of least squares using the data subjected to constant axial load ratio from 0.33 through 0.66. The dashed line, which was calculated with the same coefficient  $m$  as the solid line, represents the relation of specimens with varying axial load and roughly predict the ultimate curvatures of these specimens shown by solid circles. On the other hand, in Figs. 7(b) the thick solid line represents the calculated relation using the value  $\gamma$  of 1, which means specimens with constant axial load. Solid circles, which represent the equivalent axial load of the specimens with varying axial load, are also roughly predicted by these thick solid lines, which may lead to the conclusion that the equivalent axial load by (2) is effective.

The same procedures were applied to obtain coefficients  $m$  varying definition of deformation capacity. In other words, the coefficients  $m$  were evaluated varying strength degradation ratio  $\alpha$  from 0.7 through 1.0. Figure 8 shows relations between strength degradation ratios and coefficients  $m$ . Consequently the design equation to calculate the ultimate plastic curvature  $\phi_u$  is expressed as Eq. (9), which is a function of strength degradation ratio  $\alpha$ . Note that ultimate deflection angle  $R$  can be obtained with Eqs. (7) and (8).

$$\phi_u = \begin{cases} 2m \epsilon_p / D_c / (3 \epsilon \eta) & (1/3 > \epsilon \eta > 0) \\ 2m \epsilon_p / D_c (5 \epsilon \eta - 4) & (2/3 > \epsilon \eta > 1/3) \end{cases} \quad (9)$$

$$m = 31 - 29 \alpha$$

where,  $\epsilon \eta$  is the equivalent axial load ratio and can be obtained with Eq. (2). The maximum stress  $\sigma_p$  and the strain at the maximum point  $\epsilon_p$  of confined square core concrete can be obtained using Eqs. (3) and (4). The coefficient  $k$  was assumed to be 2/3.

## CONCLUDING REMARKS

The evaluating equation for deformation capacities determined by flexural failure was expressed as Eq. (9). The equivalent axial load ratio by Eq. (2) was found to be effective to apply Eq. (9) to columns with varying axial load.

## REFERENCE

- Architectural Institute of Japan (1990), *The design guidelines for earthquake resistant reinforced concrete buildings based on ultimate strength concept* (in Japanese)  
*Summary report on NEW RCA project in 1992* (1993), c-7) state of the art report on characteristics of confined concrete, Research center on national land development, (in Japanese)
- Kato. and Shiva (1995), J., Deformation Capacities of R/C Members under Varying Axial Load, *Summaries of Technical Papers of Annual Meeting, Architectural Institute of Japan, vol.-3, - 388* (in Japanese)